INTERFACE

rsif.royalsocietypublishing.org

Electronic and vibrational properties of carotenoids: from *in vitro* to *in vivo*

Manuel J. Llansola-Portoles, Andrew A. Pascal and Bruno Robert

Institute for Integrative Biology of the Cell (I2BC), IBITECS, CEA, CNRS, Université Paris-Saclay, 91198 Gif-sur-Yvette cedex, France

MJL-P, 0000-0002-8065-9459

Review

Check for updates

Cite this article: Llansola-Portoles MJ, Pascal AA, Robert B. 2017 Electronic and vibrational properties of carotenoids: from *in vitro* to *in vivo*. *J. R. Soc. Interface* **14**: 20170504. http://dx.doi.org/10.1098/rsif.2017.0504

Received: 12 July 2017
Accepted: 14 September 2017

Subject Category:
Reviews

Subject Areas:
biophysics

Keywords:
carotenoids, resonance Raman, vibrational properties, electronic properties

Author for correspondence:
Manuel J. Llansola-Portoles
e-mail: mjllansola@gmail.com

Carotenoids are among the most important organic compounds present in Nature and play several essential roles in biology. Their configuration is responsible for their specific photophysical properties, which can be tailored by changes in their molecular structure and in the surrounding environment. In this review, we give a general description of the main electronic and vibrational properties of carotenoids. In the first part, we describe how the electronic and vibrational properties are related to the molecular configuration of carotenoids. We show how modifications to their configuration, as well as the addition of functional groups, can affect the length of the conjugated chain. We describe the concept of effective conjugation length, and its relationship to the $S_0 \rightarrow S_2$ electronic transition, the decay rate of the S_1 energetic level and the frequency of the ν_1 Raman band. We then consider the dependence of these properties on extrinsic parameters such as the polarizability of their environment, and how this information ($S_0 \rightarrow S_2$ electronic transition, ν_1 band position, effective conjugation length and polarizability of the environment) can be represented on a single graph. In the second part of the review, we use a number of specific examples to show that the relationships can be used to disentangle the different mechanisms tuning the functional properties of protein-bound carotenoids.

1. Introduction

There are more than 700 known carotenoids in Nature, with different chemical structures, which play essential roles in biology [1,2]. Carotenoids display a number of different functions in a large range of different organisms, including bacteria, algae, plants, starfish, salmon, humans, birds, lobsters. . ., in most cases bound to protein [3]. They are mainly synthesized by photosynthetic organisms and provide vibrant natural colours—often red, orange and yellow; even blue [4]. As a general rule, other organisms only acquire carotenoid molecules (which they may then eventually modify) through their diet, although there are rare cases of animals acquiring carotenoid biosynthetic capabilities through lateral gene transfer [5,6]. Dietary intake of carotenoids by mammals is thought to be associated with reduced risks of several chronic health disorders including heart disease, age-related macular degeneration and certain cancers [7]. It has been postulated that these actions are related to the ability of carotenoids to quench reactive oxygen species [8]. Carotenoid binding to proteins can confer solubility in the aqueous cellular environment (most carotenoid molecules are highly apolar). Additionally, this binding allows tuning of their electronic and vibrational properties via the chemical properties of the binding site. The most common result of such carotenoid–protein interactions is a red-shift of the carotenoid absorption maximum—such as the shift in absorption of the carotenoid astaxanthin from 480 to 630 nm in crustacyanin, the blue carotenoid protein complex in the shell of the lobster *Homarus gammarus* or *Homarus americanus* [9–13]. Carotenoids are highly involved in the first steps of the photosynthetic process, where they assume a paradoxical double function: they play a role as light harvesters [14–18], and at the same time they act as photoprotective molecules via a number of different mechanisms,

THE ROYAL SOCIETY PUBLISHING

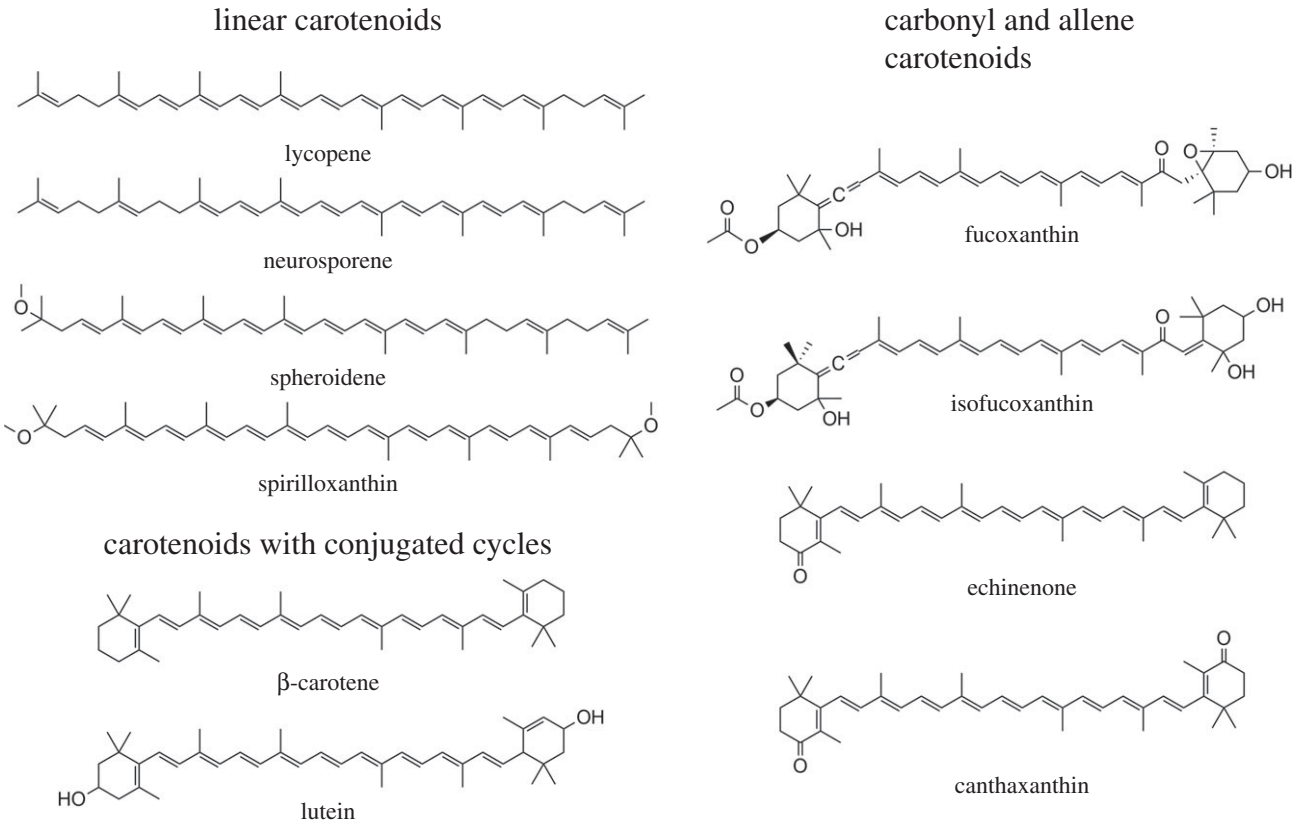

Figure 1. Structures of several carotenoids grouped as a function of their molecular complexity.

including excitation energy quenching. As light harvesters, carotenoids transfer the absorbed excited state energy to (bacterio)chlorophylls ((B)Chl); this excitation energy is eventually trapped by a reaction centre pigment–protein complex and converted into an electrical potential [19,20]. They also act as protective molecules against the photobleaching of photosynthetic organisms by quenching (B)Chl triplet states [21,22], which prevents the (B)Chl-sensitized formation of singlet state oxygen [23–29], by scavenging singlet oxygen directly [8,30] or by quenching (B)Chl singlet states [31–33]. Carotenoids have also been reported to stabilize protein structures, because many photosynthetic pigment–protein complexes do not fold properly without these molecules [34–36]. However, it is unclear whether this represents a specific function, as removing such large cofactors from a caroteno-protein structure induces the presence of a void, which is expected *per se* to dramatically influence the process of folding.

2. Molecular configuration and energy levels of carotenoids

Carotenoids are tetraterpenoid derivatives which are initially formed of eight isoprene molecules [2,37,38]. Carotenoids split into two main classes—carotenes (which are pure hydrocarbons) and xanthophylls (which contain oxygen). Carotenoids present a significant structural diversity because their carbon skeletons may vary from purely linear, including cyclic structures, or contain functional groups such as carbonyls or allenes; in each case, the grouping may be conjugated or not with the isoprenoid chain (figure 1) [1]. The electronic structure of carotenoids has been studied for more than a century, but for many years it was assumed that the lowest energy excited state in all π-electron-conjugated molecules could be reached by one-photon absorption, promoting a single electron from its highest occupied molecular orbital to its lowest unoccupied molecular orbital. Work in the early 1970s by Hudson & Kohler [39] and Schulten & Karplus [40] challenged this molecular orbital theoretical interpretation of the electronic absorption spectra for linear π-electron-conjugated polyenes (which include carotenoids). They proposed that the lowest-lying excited state, $S_1(2^1A_g^-)$, is absorption silent, displaying the same symmetry as the ground state, and that the strong absorption of carotenoids arises from a transition from the ground to the second excited state, $S_2(1^1B_u^+)$. This excited S_2 state decays by internal conversion (less than 200 fs) to the low-lying $S_1(2^1A_g^-)$ state, which itself decays to the ground state S_0 by internal conversion in several picoseconds (fluorescence occurs with extremely low yield) [41]. Other 'dark' S* states have been proposed in the vicinity of S_1 and S_2 to account for the network of relaxation pathways observed in carotenoids [42–44]. A detailed discussion of the energetic levels of carotenoids can be read in [45,46]. Carotenoids have remarkably complex excited-state dynamics, but a system of three electronic states, described in figure 2, with $S_0(1^1A_g^-)$, $S_1(2^1A_g^-)$ and $S_2(1^1B_u^+)$ electronic levels can account for most of the observed properties. The $S_0 \rightarrow S_2$ transition of carotenoids usually exhibits a characteristic three-peak structure corresponding to the lowest three vibronic bands of the electronic transition $S_0 \rightarrow S_2$, termed 0–0, 0–1 and 0–2 (figure 2). For simplicity, during the rest of this review, when we address the energy of the $S_0 \rightarrow S_2$ electronic transition, we will refer specifically to the energy of the (0–0) band.

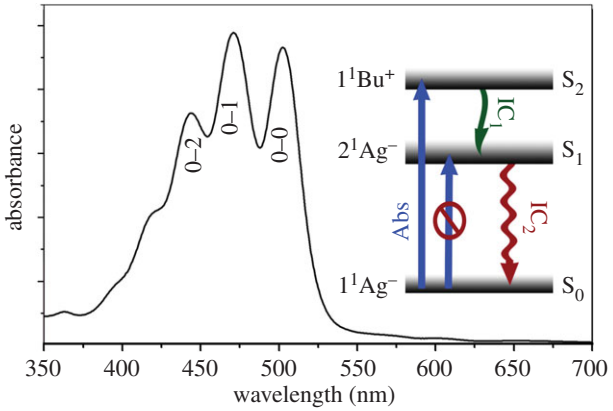

Figure 2. Typical absorption spectrum of carotenoids: lycopene at room temperature in *n*-hexane. Inset: a simplified energy diagram of carotenoids; the blue arrows represent absorption (Abs), which is forbidden for $S_0 \rightarrow S_1$, green and red arrows represent internal conversion by non-radiative decay for $S_2 \rightarrow S_1$ (IC_1) and $S_1 \rightarrow S_0$ (IC_2), respectively. There is negligible fluorescence from $S_2 \rightarrow S_0$, and no intersystem crossing to produce carotenoid triplet states.

3. A tailored vibrational technique for carotenoids

Resonance Raman is ideally suited to the study of carotenoids because the resonance coefficient of these molecules, which may reach more than six orders of magnitudes, is the highest among natural biomolecules. As a vibrational technique, resonance Raman yields direct information on the molecular properties of their electronic ground state. The resonance Raman spectra of carotenoids contain four main groups of bands, termed ν_1 to ν_4, which were observed as early as 1970 [47]. Figure 3 shows the resonance Raman spectrum of the linear carotenoid lycopene with the four major regions labelled. The most intense ν_1 band, appearing above 1500 cm^{-1}, arises from stretching vibrations of conjugated C=C double bonds [48]. Its position depends on the length of the π-electron-conjugated chain and on the molecular configuration of the carotenoid [49–53], such that an increase in conjugation length and *trans–cis* isomerization both result in an increase in ν_1 frequency (the more central the *cis* bond along the chain, the greater the effect) [49,52,53]. Additionally, the ν_1 frequency shows a linear dependence according to temperature in the 77–295 K range. This was proposed to arise from changes affecting both the vibronic coupling and the extent of π-electron delocalization in the carotenoid molecule [54]. A shift of approximately 5 cm^{-1} in the position of the ν_1 band is generally observed between 293 and 77 K [55]. The ν_2 band is actually constituted by a cluster of contributions around 1160 cm^{-1}, that arise from stretching vibrations of C–C single bonds coupled with C–H in-plane bending modes, and this region is a fingerprint for the assignment of *cis*-isomers [49,56]. The ν_3 band (approx. 1000 cm^{-1}) arises from in-plane rocking vibrations of the methyl groups attached to the conjugated chain, which are coupled with in-plane bending modes of the adjacent C–H's [48], and can be used as a fingerprint for the configuration of conjugated end-cycles [55]. Finally, the ν_4 band around 960 cm^{-1} arises from C–H out-of-plane wagging motions coupled with C=C torsional modes (out-of-plane twists of the carbon backbone) [48]. When the carotenoid conjugated system is planar, these out-of-plane modes will not be coupled with the electronic transition, and so these bands are not resonance

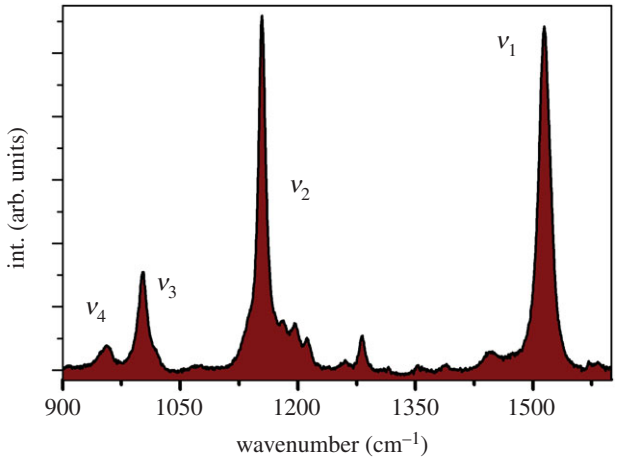

Figure 3. Typical resonance Raman spectrum of a carotenoid molecule (lycopene) in *n*-hexane. (Online version in colour.)

enhanced. However, distortions around C–C single bonds increase the coupling of these modes with the electronic transition, resulting in an increase in the structure and intensity of this band. Hence, they can be used as an indicator of such distortions (twisting) of the carotenoid backbone (see [57]). Given the apparent structural simplicity of common carotenoids such as β-carotene and lycopene, it might be supposed that their electronic and vibrational properties should be easily modelled through modern molecular physics. However, it is only recently that the calculation of these properties could be achieved with any reasonable precision, through the application of density functional theory and time-dependent density functional theory [58–62]. A full analysis of the resonance Raman spectra of carotenoids is outside the scope of this work, but it can be found in the review by Robert [63].

4. Linear carotenoids and the effect of conjugated end-cycles in solution

4.1. Effect of C=C conjugated length on electronic and vibrational properties

Araki & Murai [64] established in the early 1950s that the number of C=C double bonds in the carotenoid structure (N) is inversely related to the position of the absorption maximum, and this fundamental property has been validated by a large number of experimental studies [65–67]. This effect can be predicted with the simplest theoretical models which describe π–π* transitions [46]. The dependence of excited state energies and lifetimes of linear carotenoids on N is straightforward for linear carotenoids such as neurosporene ($N = 9$), spheroidene ($N = 10$) and lycopene ($N = 11$), where the conjugated backbone consists of a linear chain of π-electron-conjugated C=C bonds. The same linear relationship has also been demonstrated for all five low-lying excited states of linear carotenoids [68], even though the existence of three of these states is still questioned. Empirical linear relationships have been established for several series of polyene and carotenoid homologues having differing N, providing extrapolated values for the energy of their $S_0 \rightarrow S_2$ transition [46,68,69]. Extrapolating the results toward infinite polyenes and carotenoids, the experimental data give an asymptotic

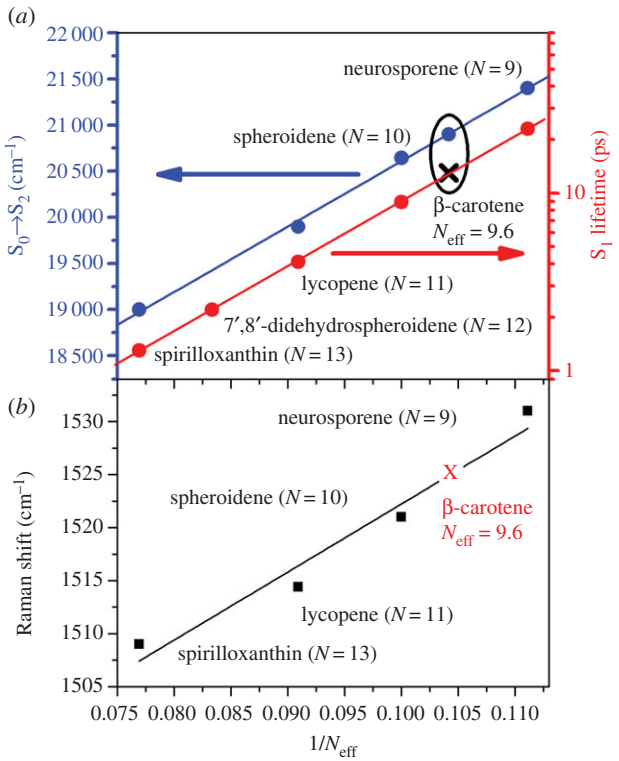

Figure 4. (*a*) Correlation between the position of the $S_0 \rightarrow S_2$ electronic transition (blue data) [76,77] and the S_1 decay rate (red data—*y* axis is in log scale) [73] with the inverse of the number of conjugated double bonds, *N*, for linear carotenoids in *n*-hexane. (*b*) Correlation between the position of the ν_1 Raman band and the inverse of the effective conjugated double bonds, N_{eff}, for linear carotenoids in *n*-hexane.

limit of 700 nm [70,71]. Linear carotenoids also show a dependence on N^{-1} for their S_1 lifetime. The pioneering work of Wasielewski & Kispert [72] demonstrated a systematic dependence of the measured S_1 lifetime on conjugation length for toluene solutions of β-carotene (8.4 ± 0.6 ps), canthaxanthin (5.2 ± 0.6 ps) and β-8′-apocarotenal (25.4 ± 0.2 ps). More recently, studies on spheroidene and linear analogues confirmed this dependence, yielding lifetimes of 400 ps ($N = 7$), 85 ps ($N = 8$), 25 ps ($N = 9$), 8.7 ps ($N = 10$), 3.9 ps ($N = 11$), 2.7 ps ($N = 12$) and 1.1 ps (13) [73]. A similar dependence was found for a β-carotene series (although with slightly different values): 282 ps ($N = 7$), 96 ps ($N = 8$), 52 ps ($N = 9$) and 8.1 ps ($N = 11$) [68]. Finally, the vibrational properties, and specifically the position of the ν_1 Raman band, are also dependent on the conjugation length (*N*) [69,74,75]. Figure 4 displays the linear correlation between the ν_1 position and N^{-1} for the linear carotenoids neurosporene ($N = 9$), spheroidene ($N = 10$), lycopene ($N = 11$) and spirilloxanthin ($N = 13$) in *n*-hexane. As for their S_1 decay rates and the energy of their $S_0 \rightarrow S_2$ transition, the measurement of the ν_1 Raman band can give accurate values for the conjugation chain length *N* of these molecules.

This elegant linear relationship between the *nominal* conjugation length *N* (that assumed from the chemical structure) and the $S_0 \rightarrow S_2$ electronic transition, S_1 decay rate and ν_1 Raman band is not always readily followed by carotenoids containing chemical groups, such as conjugated end-cycles, β-rings, ketones and allene groups. In carbonyl carotenoids the presence of a conjugated C=O group extends the conjugated part of the chromophore, resulting in a shift of the absorption transition to longer wavelengths. Aryl-carotenoids and linear carotenoids with conjugated end-cycles (the class which has been the most extensively studied up to now) behave, from the point of view of their absorption, vibrational and photochemical properties, as carotenoids with shorter conjugation length than expected. This was proposed to arise from a decrease in orbital overlap between the π-orbital of the ring double bond and those of the polyene chain, as steric hindrance results in twisting of the conjugated end-cycles out of the conjugated plane [78]. Although the conjugated end-cycle contributes to the conjugation chain length [76,79], it extends it by the equivalent of only 0.3 of a C=C bond. For instance, β-carotene, instead of showing the properties of a carotenoid with 11 C=C bonds (as would be expected from its structure), presents the spectroscopic properties of a carotenoid with only 9.6 C=C bonds [75,76]. This value was termed the *effective* conjugation length (N_{eff}), as it accounts for the carotenoids' electronic and vibrational properties. Studies on a series of β-carotene derivatives with different chain lengths showed that these follow a similar relationship to linear ones, but shifted due to the partial conjugation of their end-rings [75]. Similar results were also observed for aryl-carotenoids [76]. The N_{eff} value works exceedingly well for predicting the electronic properties of carotenoids—their absorption position, but also their S_1 decay rate. The relationship between the $S_0 \rightarrow S_2$ electronic transition and the S_1 decay rate with the inverse of *N* is displayed in figure 4 for linear carotenoids (where the effective and nominal conjugation length is the same) as well as for β-carotene ($N_{eff} = 9.6$) in *n*-hexane (blue line). For both relationships, the N_{eff} value calculated for β-carotene indicates that it obeys the same trend as linear carotenoids, once its effective conjugation is taken into account. Similarly, the correlation between the frequency of the ν_1 Raman band with the inverse of the effective carotenoid conjugation length (N_{eff}) is also well established in the literature [69,74,75]. Using β-carotene to illustrate this, the measured ν_1 frequency of 1525 cm^{-1} gives the same value of $N_{eff} = 9.6$ as that obtained using the other methods, demonstrating that they are equivalent. For simplicity, only β-carotene is plotted here, but this concept can be extended to all carotenoids with conjugated end-cycles, as well as to aryl-carotenoid molecules.

4.2. Effect of environment polarizability

The effect of solvent properties, specifically the refractive index, *n*, and dielectric constant, ε, on the position of the absorption transition of carotenoid molecules has been studied extensively [64,80–87]. The position of the $S_0 \rightarrow S_2$ electronic transition in solution depends on the solvent polarizability defined as $R(n) = (n^2 - 1)/(n^2 + 2)$, *n* being the refractive index of the solvent. For linear carotenoids the $S_0 \rightarrow S_2$ transition shifts to a longer wavelength as the refractive index increases [86] due to dispersive interactions between the solvent environment and the large transition dipole moment of the carotenoid [86]. A significant linear correlation was found between the frequency of the ν_1 Raman band and the polarizability of the solvent for different linear carotenoids (including those with conjugated end-cycles), proving an influence of the solvent polarizability on the carotenoid ground state [75]. Figure 5*a*,*b* represents a practical example of the polarizability effect on the absorption spectra and ν_1 Raman band for lycopene in *n*-hexane and carbon disulfide. Figure 5*c* plots the correlation between the $S_0 \rightarrow S_2$ electronic transition and the polarizability of the

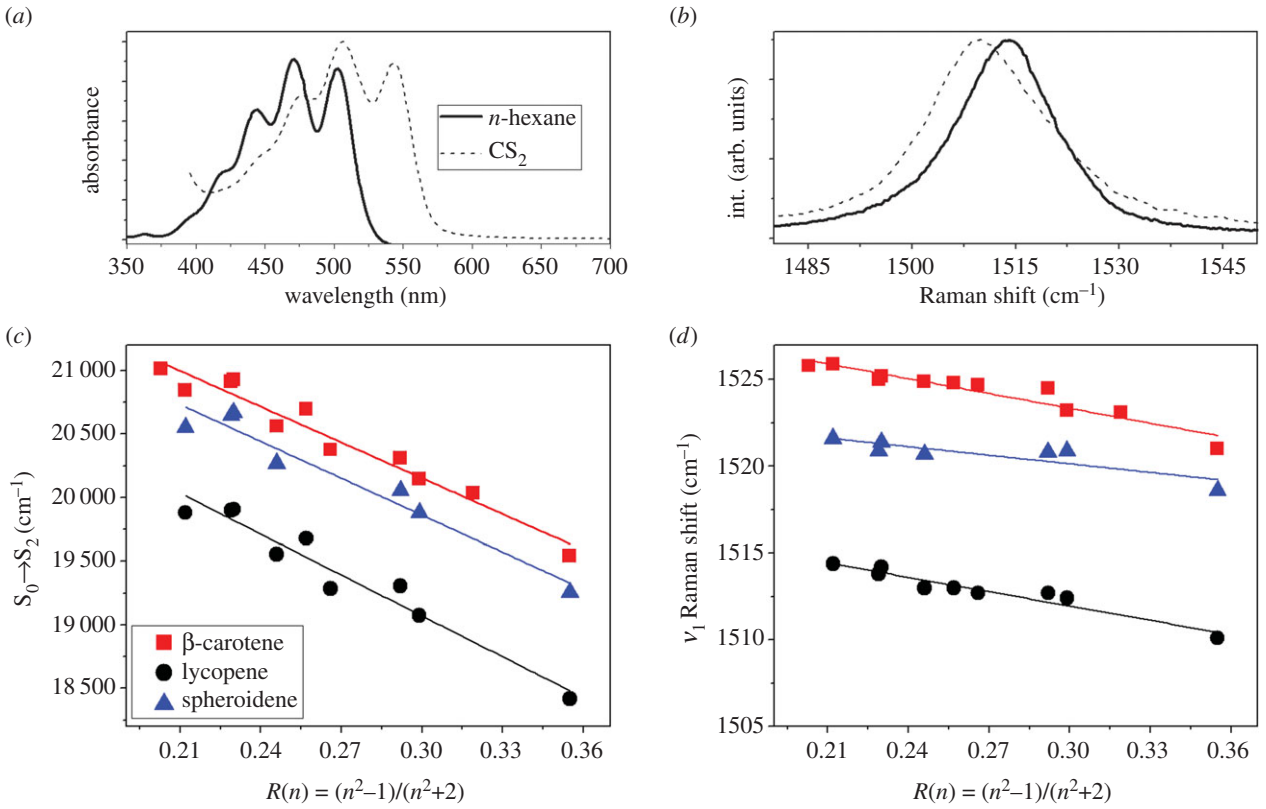

Figure 5. (*a*) Absorption red-shift of a typical linear carotenoid (lycopene) in solvents with different polarizability. (*b*) ν_1 Raman band shift of lycopene in solvents with different polarizability. (*c*) Correlation between the $S_0 \rightarrow S_2$ electronic transition and solvent polarizability for β-carotene, lycopene and spheroidene. (*d*) Correlation between the ν_1 band position and solvent polarizability for β-carotene, lycopene and spheroidene [75].

solvent for β-carotene, lycopene and spheroidene. It illustrates a clear linear relationship that can be extended to a great variety of linear carotenoids. Figure 5*d* plots the correlation between the position of the ν_1 Raman band and the polarizability of the solvent for β-carotene, lycopene and spheroidene. Again, this linear relationship extends to a large variety of carotenoids (linear, linear with conjugated end-cycles, aryl-carotenoids and in this case those with allene groups) [75,88]. The ν_1 Raman band reflects polarizability-induced changes in the ground state only, while the absorption shift results from the combined effects on both S_0 and S_2. It is also of note that the dependence on polarizability appears to be similar for all carotenoid molecules and exhibits comparable trends, albeit the slopes are not identical.

4.3. Combining intrinsic and extrinsic effects: $S_0 \rightarrow S_2$, ν_1 Raman band, polarizability of the environment (R), and N_{eff}

In the previous sections, we have seen that the energy of the $S_0 \rightarrow S_2$ electronic transition and the frequency of the ν_1 Raman band are linearly dependent on intrinsic factors, namely $1/N_{eff}$, and on environmental factors, namely the polarizability of the environment. As all these properties are linked by linear dependences, it is possible to conceive a graph containing all the information discussed above, plotting the linear relationship between the position of the carotenoid $S_0 \rightarrow S_2$ electronic transition and the frequency of its ν_1 Raman band [51,69]. As both of these parameters strictly depend on N_{eff}, they present an excellent correlation for all the carotenoids studied, as shown in figure 6. In addition, the effect of polarizability on the effective conjugation length of these molecules can easily be distinguished, as it results in a shift of this straight line (e.g. between the blue and orange lines in figure 6). For simplicity, we will refer to this type of plot, which relates the position of the electronic transition to the frequency of the ν_1 Raman band at room temperature, as the MP graph (from the first author of the original paper in 2013, Mendes-Pinto) [75]. In the MP graph in figure 6, we have removed most of the experimental points obtained for different solvents, showing only those for *n*-hexane (blue line and circles), a common solvent with low polarizability (0.299), and for carbon disulfide (orange line), a solvent with high polarizability (0.355). Each arrow represents the MP relationship for a single carotenoid species according to the polarizability of the environment, and illustrates the shift from the blue to the orange line. This graph may be used to disentangle the different mechanisms underlying the tuning of the energy of the $S_0 \rightarrow S_2$ transition observed in complex media, and in particular in proteins or *in vivo*.

5. Carotenoids containing carbonyl and allene groups in solution

Carotenoids display a vast structural variability, and the presence of additional chemical groups makes analysis of their electronic behaviour increasingly difficult. For example, the presence of carbonyl or allene groups can influence the effective conjugation length or S_2 excited state; however, this is in a different way from that observed in linear or linear with conjugated end-cycle carotenoids. Figure 7 illustrates this, as it displays an MP graph where two keto-carotenoid

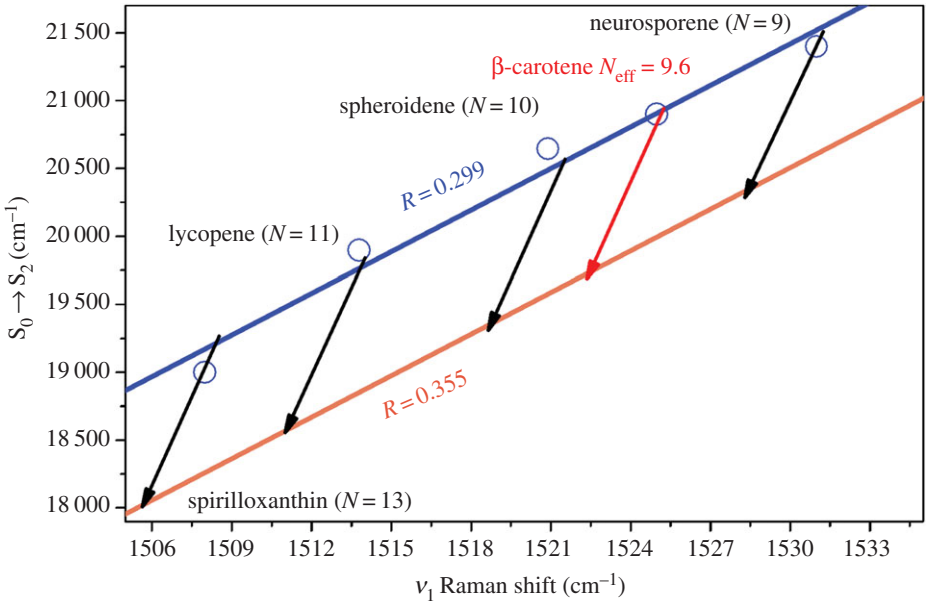

Figure 6. MP graph showing the correlation between the position of the $S_0 \rightarrow S_2$ electronic transition and the ν_1 Raman band, as a function of solvent polarizability at room temperature, for spirilloxanthin, lycopene, spheroidene, β-carotene and neurosporene.

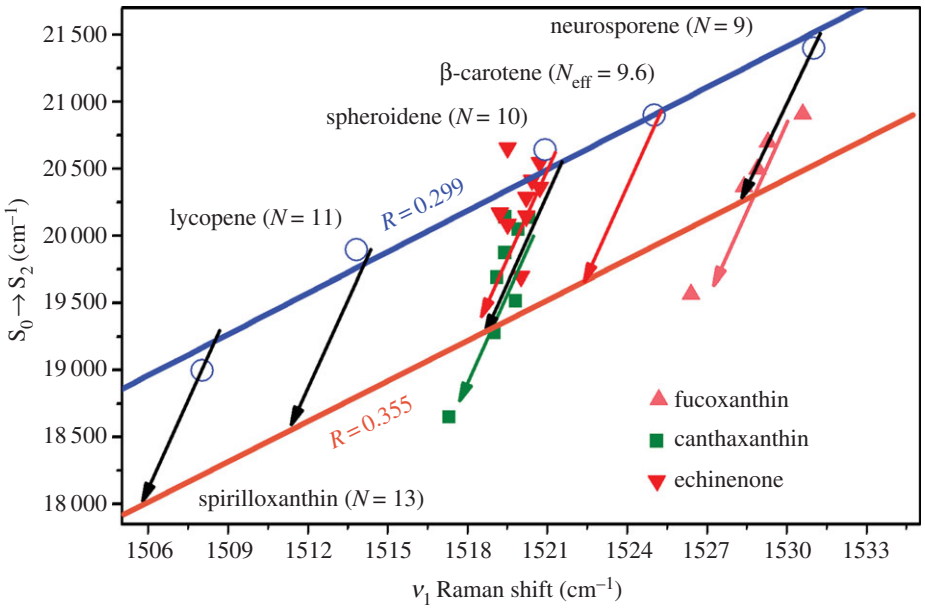

Figure 7. Correlation between the position of the $S_0 \rightarrow S_2$ electronic transition and the $\nu 1$ band frequency for different N_{eff} and polarizability of the environment for linear carotenoids at room temperature. The values of fucoxanthin (pink triangles), 3-hydroxyechinenone (red triangles) and canthaxanthin (green squares) are plotted for different solvents according to [88,89]. For simplicity, the name of the solvent is not written and the arrows of the corresponding colour mark the tendency with increasing polarizability from *n*-hexane to carbon disulfide.

molecules, namely echinenone and canthaxanthin [89], as well as one allene carotenoid, fucoxanthin [88], are represented. Echinenone (downward red triangles) differs from β-carotene by one C=O on one of its rings, and presents an N_{eff} slightly longer than that of β-carotene. However, canthaxanthin, which contains one C=O on each of its two rings, is clearly off the blue line. The introduction of a keto group in the carotenoid thus has a complex effect on its electronic structure. A similar effect is observed with fucoxanthin, a more complicated carotenoid containing both keto groups and an allene group. Fucoxanthin has seven nominal double bonds plus an allene group and a keto group. The representation of the pair (ν_1, $S_0 \rightarrow S_2$) for fucoxanthin (upward pink triangles) shows how it falls off the line for N_{eff}, also indicating a perturbation of its S_2 excited state.

6. Carotenoids in photosynthetic protein complexes

The electronic properties of carotenoid molecules underlie their multiple functions throughout Nature. In biological systems, carotenoids are generally present in highly anisotropic environments and most often bound to proteins, and their properties are tuned by these complex binding sites. In this review we restrict ourselves to the scope of carotenoids present in well-defined environments, and it is mainly in photosynthesis that the environment of the different carotenoids is precisely known (due to the existence of three-dimensional structures for a large number of photosynthetic pigment-binding proteins). In light-harvesting (LH) complexes, carotenoids perform both LH and photoprotective

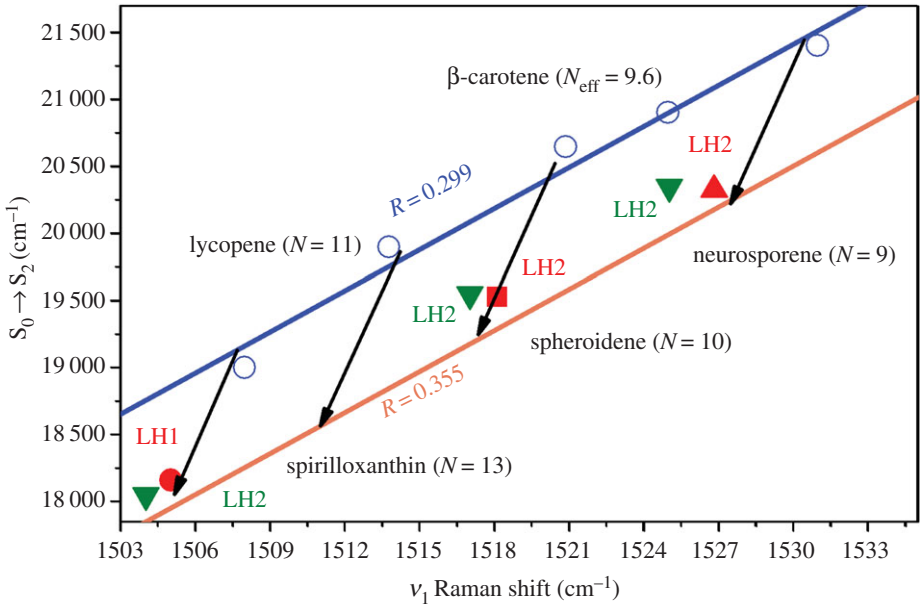

Figure 8. Correlation between the position of the $S_0 \rightarrow S_2$ electronic transition and the ν_1 Raman band for spirilloxanthin, spheroidene and neurosporene, in *n*-hexane (blue circles) and bound to LH proteins (results reproduced from Mendes-Pinto *et al.*, red symbols [75], and Dilbeck *et al.*, green symbols [33]). For comparison, the relationship between carotenoids of different conjugation length in *n*-hexane (blue line) and CS_2 (orange line) is added, as well as the relationship as a function of solvent polarizability (black arrows) [75].

roles. The electronic properties of several carotenoids in photosynthetic proteins have been studied extensively, including (i) linear molecules in purple bacteria, spheroidene, neurosporene and spirilloxanthin [33,90,91], (ii) cyclic molecules, β-carotene, lutein and xanthophyll cycle pigments in higher plants [92–94] and cyanobacteria [32], and (iii) carbonyl carotenoids in marine algae, 3-hydroyechinenone [95,96], peridinin [60,97], fucoxanthin [98,99] and fucoxanthin derivatives [88]. In the following sections, we will describe practical cases where the relationships obtained above are useful for conveying new information; we also discuss their current limitations.

6.1. Linear carotenoids in purple bacteria

LH pigment–protein complexes from purple photosynthetic bacteria can bind many different carotenoids, with significant variations observed not only between bacterial species but also for the same species in different habitats [90]. These carotenoids can have different functions depending on their configuration and environment, either as auxiliary LH molecules [100,101] or as photoprotective species quenching Chl exited states [33,90,91]. In native LH pigment–protein complexes, spheroidene and neurosporene bind to LH2 from *Rhodobacter sphaeroides*, strains 2.4.1 (grown anaerobically) and G1C, respectively, whereas spirilloxanthin is present in LH1 from *Rhodospirillum rubrum* strain S1 [90,91,102]. The correlation between the ν_1 Raman band and the position of the $S_0 \rightarrow S_2$ transition for these carotenoid-bound proteins was compared with the correlation found for *in vitro* carotenoids (figure 8, red symbols). The position of the pairs of values (ν_1, $S_0 \rightarrow S_2$) for LH-bound spheroidene, neurosporene and spirilloxanthin clearly follows the correlation seen when varying the polarizability of the solvent for the corresponding isolated carotenoid. These results suggest that the average polarizability of the protein binding pocket is the dominant factor for tuning the position of the $S_0 \rightarrow S_2$ transition upon binding to their LH protein host. This average polarizability, which is nearly identical for the three proteins, corresponds to a value, $R(n)$, of about 0.334, slightly lower than that found in carbon disulfide ($R = 0.355$). This value is very high, and can be explained by the fact that LH-bound carotenoids are in close contact with (B)Chl molecules, which may provide them with a highly polarizable environment [103]. Given that the carotenoid in each case occupies an equivalent binding position in these homologous LH proteins, the binding pocket is also expected to exhibit similar electrostatic properties, as observed here [75]. Similar results were found by Dilbeck *et al.* [33] for six LH2 proteins from genetically modified strains of the purple photosynthetic bacterium *Rhodobacter (Rb.) sphaeroides*. It was again found that the shift in the ν_1 Raman band and the absorption spectrum for the studied LH2-bound carotenoids (neurosporene, spheroidene, lycopene, spirilloxanthin, ketospirilloxanthin or diketospirilloxanthin) could be explained by the polarizability of the environment alone. Figure 8 compares the results obtained for neurosporene, spheroidene and spirilloxanthin in the two studies described here. Both studies describe a similar behaviour of the carotenoids in LH1 and LH2 from purple bacteria, down-shifting their energy levels due to the polarizability of their binding environment. The data obtained by Dilbeck *et al.* (green symbols) are slightly red-shifted by approximately 1–2 cm^{-1} from the results obtained by Mendes-Pinto *et al.* (red symbols), but this should be considered as within experimental error because they were obtained in different set-ups.

6.2. Cyclic carotenoids in higher plants and cyanobacteria

The use of the relationship described here is not only applicable to changes caused by the polarizability of the environment. The LHCII protein, the major LH protein from higher plants, binds two lutein molecules which exhibit electronic transitions at different positions. LHCII is a very complex protein–pigment complex, which assembles into a trimer in the photosynthetic membrane, with each monomer

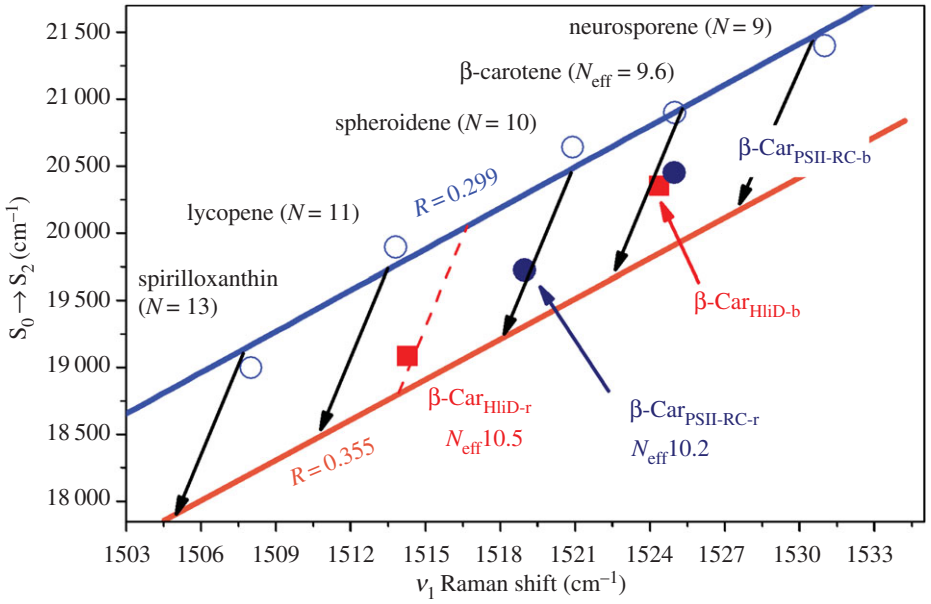

Figure 9. Correlation between the position of the $S_0 \rightarrow S_2$ electronic transition and the $\nu 1$ Raman band for β-carotenes in PSII-RC (dark blue circles) and HliD proteins (red squares) at room temperature. For comparison, the relationship between carotenoids of different conjugation lengths in the same solvent (*n*-hexane) is added as well as the relationship as a function of solvent polarizability (black arrows). The $\beta\text{-Car}_{\text{PSII-RC-b}}$ point corresponds to the blue-absorbing β-carotene in PSII-RC, the $\beta\text{-Car}_{\text{PSII-RC-r}}$ point corresponds to the red-absorbing β-carotene in PSII-RC, the $\beta\text{-Car}_{\text{HliD-b}}$ point corresponds to the blue-absorbing β-carotene in HliD, and the $\beta\text{-Car}_{\text{HliD-r}}$ point corresponds to the red-absorbing β-carotene in HliD.

containing two lutein molecules whose binding sites are related by pseudo-symmetry. Whereas in LHCII monomers both luteins absorb at 495 nm, in LHCII trimers one lutein (lut_1) absorbs at 495 nm whereas the second one (lut_2) is shifted to 510 nm [92,93]. Plotting the lut_1 pair of (ν_1, $S_0 \rightarrow S_2$) values on an MP plot shows that the position of its electronic transition is mainly governed by the polarizability of its protein binding site (as is the case for both luteins in LHCII monomers). Indeed, this pair strictly obeys the correlation obtained for lutein according to the solvent refractive index. However, the (ν_1, $S_0 \rightarrow S_2$) pair for lut_2 shows that the energy shifts between the blue- and the red-absorbing lutein molecules are not induced by a variation in polarizability of their binding sites. Instead, the lut_2 values suggest that the conjugated chain of the carotenoid is increased by nearly one C=C double bond at constant polarizability. The apparent length of the conjugated chain for lutein in solvent (and for lut_1 in LHCII) is 9.3—as discussed above, the ring is only partially conjugated as steric hindrance causes rotation of the ring out of the conjugated plane. On the other hand, N_{eff} for the red-absorbing lut_2 in LHCII is approximately 10. This increase in N_{eff} was suggested to be due to rotation of the β-ring back towards a planar conformation, resulting in a gain in conjugation length [55]. A similar effect was observed with the two β-carotene molecules in the photosystem II reaction centre, PSII-RC, which also displays shifted absorption [104–106]. Plotting the (ν_1, $S_0 \rightarrow S_2$) pair for each of these molecules (figure 9) shows that, while the blue-absorbing β-carotene fits on the line obtained for β-carotene in different solvents, the values obtained for the red-absorbing β-carotene suggests a sizeable increase in the apparent conjugation length (calculated as approx. 10.2). Analysis of the available three-dimensional structures for both LHCII and PSII-RC revealed the presence, in both cases, of an aromatic sidechain forcing the ring of the red-absorbing carotenoid back into the conjugated plane through steric hindrance [55]. In helix high-light-inducible proteins (Hlips) from cyanobacteria (HliD), the two bound β-carotenes display even more distinct electronic transitions: $\beta\text{-Car}_{\text{HliD-b}}$ presents $S_0 \rightarrow S_2$ at 498 nm whereas $\beta\text{-Car}_{\text{HliD-r}}$ exhibits $S_0 \rightarrow S_2$ at 525 nm [32,94]. Plotting (ν_1, $S_0 \rightarrow S_2$) pairs on an MP graph for these two carotenes again shows that, while the pair corresponding to the blue $\beta\text{-Car}_{\text{HliD-b}}$ lies on the line obtained for β-carotene in solvents, the red-absorbing one ($\beta\text{-Car}_{\text{HliD-r}}$) deviates from this line. Again it was concluded that the electronic properties of the blue carotene are tuned by the polarizability of its protein binding site, while the red-absorbing molecule must display a longer effective conjugated length, as well as being present in an environment of relatively high polarizability. It was proposed in this case that the effective length of $\beta\text{-Car}_{\text{HliD-r}}$ lies between 10.5 and 10.6 C=C, and the polarizability of its binding site is either in the first case very high, similar to carbon disulfide, or similar to toluene in the second case.

6.3. Proteins containing carbonyl or allene carotenoids

It is difficult to extract similar information for carbonyl and allene carotenoids in biological environments as they do not follow the same patterns as the simpler carotenoids discussed above. However, comparison with their properties in different solvents can nevertheless be useful in addressing their properties in photosynthetic proteins. Orange carotenoid protein (OCP) is a cyanobacterial photoactive protein, involved in the photoprotection of these photosynthetic organisms against intense illumination [107,108]. The bound carotenoid 3-hydroxyechinenone (spectroscopically indistinguishable from echinenone) spans its N-terminal and C-terminal domains [109]. The orange-coloured OCPo before illumination is converted to red OCPr upon illumination with intense blue-green light, and this is linked to a change in configuration of the 3′-hydroxyechinenone [110]. The pairs (ν_1, $S_0 \rightarrow S_2$) were

plotted on an MP graph for this carotenoid in several solvents, and compared with the values obtained for OCPo and OCPr. The data for OCPr are consistent with a carotenoid of similar effective conjugation length to isolated 3-hydroxyechinenone, in a highly polarizable environment. Thus the OCPr carotenoid is in a planar, *all-trans* conformation. The OCPo pair indicates that the effective conjugation length of orange 3-hydroxyechinenone ($N_{\mathrm{eff}} \cong 9$) is much shorter than isolated echinenone in solvents ($N_{\mathrm{eff}} \cong 10$), although resonance Raman spectra of this molecule otherwise show it is in an *all-trans configuration* [89]. These results, together with density functional theory calculations of three isomers of echinenone and canthaxanthin, suggest two possible mechanisms for the OCPo to OCPr transition. An s-*cis* to s-*trans* isomerization of the carotenoid end-cycle would increase the relative conjugation of this ring; alternatively, bending both of the echinenone rings would bring them from out of the conjugated C=C plane in the OCPo form and into the C=C plane in the OCPr form [89].

Our last example concerns an allene carotenoid, the isofucoxanthin-like carotenoid (Ifx-l) found in the LH complex of *Chromera velia* [88]. This antenna protein contains, in addition to chlorophyll *a* and linear carotenoids, two Ifx-l with different configurations, with absorption bands located at 515 and 548 nm, respectively. The measured (ν_1, $S_0 \rightarrow S_2$) values for the two protein-bound Ifx-l molecules were compared on an MP graph with a series of data obtained for isolated Ifx-l in several solvents (*n*-hexane, cyclohexane, diethyl ether, toluene, acetonitrile and carbon disulfide). Even though allenic carotenoids do not behave exactly as linear carotenoids, it was nevertheless possible from such a comparison to conclude that the electronic absorption of the blue-absorbing Ifx-l is mainly tuned by the polarizability of its environment, while the red-absorbing one largely deviates from the solvent-derived relationship. The electronic transition of this carotenoid is approximately 900 cm^{-1} below that of the blue Ifx-l, even though they both exhibit the same ν_1 Raman frequency. It was concluded that the absorption of the red-absorbing Ifx-l_2 presents at best a weak charge transfer character [111]. Nonetheless, these results suggest that the shift in energy of the transition of the red-absorbing Ifx-l arises from a change in the excited state structure only [88].

7. Conclusion

In the first part of this review, we address the different electronic and vibrational properties of carotenoids and discuss the influence of the presence of additional, conjugated groups on these properties. For isolated carotenoids, we introduce the concept of effective conjugation length, and how this parameter is related to their $S_0 \rightarrow S_2$ electronic transitions, the decay rate of the S_1 energetic level and the frequency of the vibrational ν_1 Raman band. We then describe how these parameters depend not only on intrinsic parameters such as effective conjugation length, but also on extrinsic (environmental) parameters such as the polarizability of their environment. We go on to explain how all this information can be represented on a single (MP) graph. The usefulness of this type of plot is then illustrated in the second part of the review. We give several examples of protein-bound carotenoids, and show how the MP graph can be used to disentangle the various parameters responsible for tuning of their functional properties.

Data accessibility. This article has no additional data.

Competing interests. We declare we have no competing interests.

Funding. This work was supported by French Infrastructure for Integrated Structural Biology (FRISBI).

References

1. Britton G, Liaaen-Jensen S, Pfander H. 2008 *Carotenoids, volume 4: natural functions*. Basel, Switzerland: Birkhäuser.
2. Britton G. 1995 Structure and properties of carotenoids in relation to function. *FASEB J.* **9**, 1551–1558.
3. Vershinin A. 1999 Biological functions of carotenoids—diversity and evolution. *Biofactors* **10**, 99–104. (doi:10.1002/biof.5520100203)
4. Isler O, Gutmann H, Solms U. 1971 *Carotenoids*. Basel, Switzerland: Birkhäuser.
5. Altincicek B, Kovacs JL, Gerardo NM. 2012 Horizontally transferred fungal carotenoid genes in the two-spotted spider mite *Tetranychus urticae*. *Biol. Lett.* **8**, 253–257. (doi:10.1098/rsbl.2011.0704)
6. Moran NA, Jarvik T. 2010 Lateral transfer of genes from fungi underlies carotenoid production in aphids. *Science* **328**, 624–627. (doi:10.1126/science.1187113)
7. Cooper DA, Eldridge AL, Peters JC. 1999 Dietary carotenoids and certain cancers, heart disease, and age-related macular degeneration: a review of recent research. *Nutr. Rev.* **57**, 201–214. (doi:10.1111/j.1753-4887.1999.tb06944.x)
8. Krinsky NI. 1971 Function. In *Carotenoids* (eds O Isler, H Gutmann, U Solms), pp. 669–716. Basel, Switzerland: Birkhauser.
9. Cianci M, Rizkallah PJ, Olczak A, Raftery J, Chayen NE, Zagalsky PF, Helliwell JR. 2002 The molecular basis of the coloration mechanism in lobster shell: β-crustacyanin at 3.2-Å resolution. *Proc. Natl Acad. Sci. USA* **99**, 9795–9800. (doi:10.1073/pnas.152088999)
10. Ilagan RP, Shima S, Melkozernov A, Lin S, Blankenship RE, Sharples FP, Hiller RG, Birge RR, Frank HA. 2004 Spectroscopic properties of the main-form and high-salt peridinin–chlorophyll *a* proteins from *Amphidinium carterae*. *Biochemistry* **43**, 1478–1487. (doi:10.1021/bi0357964)
11. Buchwald M, Jencks WP. 1968 Properties of the crustacyanins and the yellow lobster shell pigment. *Biochemistry* **7**, 844–859. (doi:10.1021/bi00842a043)
12. Britton G *et al.* 1997 Carotenoid blues: structural studies on carotenoproteins. *Pure Appl. Chem.* **69**, 2075. (doi:10.1351/pac199769102075)
13. Weesie RJ, Merlin JC, De Groot HJM, Britton G, Lugtenburg J, Jansen FJHM, Cornard JP. 1999 Resonance Raman spectroscopy and quantum chemical modeling studies of protein–astaxanthin interactions in α-crustacyanin (major blue carotenoprotein complex in carapace of lobster, *Homarus gammarus*). *Biospectroscopy* **5**, 358–370. (doi:10.1002/(SICI)1520-6343(1999)5:6<358::AID-BSPY5>3.0.CO;2-1)
14. Goedheer JC. 1969 Energy transfer from carotenoids to chlorophyll in blue-green, red and green algae and greening bean leaves. *Biochim. Biophys. Acta* **172**, 252–265. (doi:10.1016/0005-2728(69)90068-1)
15. Govindjee, Govindjee R. 1975 Bioenergetics of photosynthesis. In *Cell biology* (ed. Govindjee), pp. 2–50. New York, NY: Academic Press.
16. Cogdell RJ. 1978 Carotenoids in photosynthesis. *Phil. Trans. R. Soc. Lond. B* **284**, 569–579. (doi:10.1098/rstb.1978.0090)
17. Frank HA, Christensen RL. 1995 Singlet energy transfer from carotenoids to bacteriochlorophylls. In *Anoxygenic photosynthetic bacteria* (eds RE Blankenship, MT Madigan, CE Bauer), pp. 373–384. Dordrecht, The Netherlands: Springer.
18. Scholes GD, Fleming GR, Olaya-Castro A, van Grondelle R. 2011 Lessons from nature about solar

light harvesting. *Nat. Chem.* **3**, 763–774. (doi:10.1038/nchem.1145)

19. Kirmaier C, Holten D. 1987 Primary photochemistry of reaction centers from the photosynthetic purple bacteria. *Photosynth. Res.* **13**, 225–260. (doi:10.1007/bf00029401)
20. Blankenship RE, Madigan MT, Bauer CE. 1995 *Anoxygenic photosynthetic bacteria*. Dordrecht, The Netherlands: Kluwer Academic Publishers.
21. Monger TG, Cogdell RJ, Parson WW. 1976 Triplet states of bacteriochlorophyll and carotenoids in chromatophores of photosynthetic bacteria. *Biochim. Biophys. Acta* **449**, 136–153. (doi:10.1016/0005-2728(76)90013-X)
22. Niedzwiedzki DM, Blankenship RE. 2010 Singlet and triplet excited state properties of natural chlorophylls and bacteriochlorophylls. *Photosynth. Res.* **106**, 227–238. (doi:10.1007/s11120-010-9598-9)
23. Foote CS. 1968 Mechanisms of photosensitized oxidation. *Science* **162**, 963–970. (doi:10.1126/science.162.3857.963).
24. Krinsky NI. 1968 The protective function of carotenoid pigments. In *Photophysiology Iii* (ed. AC Giese), pp. 123–195. New York, NY: Academic Press.
25. Goodwin TW. 1976 *Chemistry and biochemistry of plant pigments*. New York, NY: Academic Press.
26. Renger G, Wolff C. 1977 Further evidence for dissipative energy migration via triplet states in photosynthesis. The protective mechanism of carotenoids in *Rhodopseudomonas spheroides* chromatophores. *Biochim. Biophys. Acta* **460**, 47–57. (doi:10.1016/0005-2728(77)90150-5)
27. Boucher F, Van der Rest M, Gingras G. 1977 Structure and function of carotenoids in the photoreaction center from *Rhodospirillum rubrum*. *Biochim. Biophys. Acta* **461**, 339–357. (doi:10.1016/0005-2728(77)90224-9)
28. Cogdell RJ, Frank HA. 1987 How carotenoids function in photosynthetic bacteria. *Biochim. Biophys. Acta* **895**, 63–79. (doi:10.1016/S0304-4173(87)80008-3)
29. Frank HA, Cogdell RJ. 1993 The photochemistry and function of carotenoids in photosynthesis. In *Carotenoids in photosynthesis* (eds AJ Young, G Britton), pp. 252–326. Dordrecht, The Netherlands: Springer.
30. Foote CS, Chang YC, Denny RW. 1970 Chemistry of singlet oxygen. X. Carotenoid quenching parallels biological protection. *J. Am. Chem. Soc.* **92**, 5216–5218. (doi:10.1021/ja00720a036)
31. Ruban AV *et al.* 2007 Identification of a mechanism of photoprotective energy dissipation in higher plants. *Nature* **450**, 575–578. (doi:10.1038/nature06262)
32. Staleva H, Komenda J, Shukla MK, Šlouf V, Kaňa R, Polívka T, Sobotka R. 2015 Mechanism of photoprotection in the cyanobacterial ancestor of plant antenna proteins. *Nat. Chem. Biol.* **11**, 287–291. (doi:10.1038/nchembio.1755)
33. Dilbeck PL, Tang Q, Mothersole DJ, Martin EC, Hunter CN, Bocian DF, Holten D, Niedzwiedzki DM. 2016 Quenching capabilities of long-chain carotenoids in light-harvesting-2 complexes from *Rhodobacter sphaeroides* with an engineered carotenoid synthesis pathway. *J. Phys. Chem. B* **120**, 5429–5443. (doi:10.1021/acs.jpcb.6b03305)
34. Lang HP, Hunter CN. 1994 The relationship between carotenoid biosynthesis and the assembly of the light-harvesting LH2 complex in *Rhodobacter sphaeroides*. *Biochem. J.* **298**, 197–205. (doi:10.1042/bj2980197)
35. Yamamoto H, Bassi R. 1996 Carotenoids: localization and function. In *Oxygenic photosynthesis: the light reactions* (eds DR Ort, CF Yocum), pp. 539–563. Dordrecht, The Netherlands: Kluwer Academic Publishers.
36. Sandonà D, Croce R, Pagano A, Crimi M, Bassi R. 1998 Higher plants light harvesting proteins. Structure and function as revealed by mutation analysis of either protein or chromophore moieties. *Biochim. Biophys. Acta* **1365**, 207–214. (doi:10.1016/S0005-2728(98)00068-1)
37. Maiani G *et al.* 2009 Carotenoids: actual knowledge on food sources, intakes, stability and bioavailability and their protective role in humans. *Mol. Nutr. Food Res.* **53**, S194–S218. (doi:10.1002/mnfr.200800053)
38. Walter MH, Strack D. 2011 Carotenoids and their cleavage products: biosynthesis and functions. *Nat. Prod. Rep.* **28**, 663–692. (doi:10.1039/C0NP00036A)
39. Hudson BS, Kohler BE. 1972 A low-lying weak transition in the polyene A,Ω-diphenyloctatetraene. *Chem. Phys. Lett.* **14**, 299–304. (doi:10.1016/0009-2614(72)80119-2)
40. Schulten K, Karplus M. 1972 On the origin of a low-lying forbidden transition in polyenes and related molecules. *Chem. Phys. Lett.* **14**, 305–309. (doi:10.1016/0009-2614(72)80120-9)
41. Frank HA, Christensen RL. 2008 Excited electronic states, photochemistry and photophysics of carotenoids. In *Carotenoids: volume 4: natural functions* (eds G Britton, S Liaaen-Jensen, H Pfander), pp. 167–188. Basel, Switzerland: Birkhäuser.
42. Polívka T, Sundström V. 2009 Dark excited states of carotenoids: consensus and controversy. *Chem. Phys. Lett.* **477**, 1–11. (doi:10.1016/j.cplett.2009.06.011)
43. Buckup T, Motzkus M. 2014 Multidimensional time-resolved spectroscopy of vibrational coherence in biopolyenes. *Annu. Rev. Phys. Chem.* **65**, 39–57. (doi:10.1146/annurev-physchem-040513-103619)
44. Balevičius V, Abramavicius D, Polívka T, Galestian Pour A, Hauer J. 2016 A unified picture of S* in carotenoids. *J. Phys. Chem. Lett.* **7**, 3347–3352. (doi:10.1021/acs.jpclett.6b01455)
45. Robert B. 1999 The electronic structure, stereochemistry and resonance Raman spectroscopy of carotenoids. In *The photochemistry of carotenoids* (eds HA Frank, AJ Young, G Britton, RJ Cogdell), pp. 189–201. Dordrecht, The Netherlands: Springer.
46. Christensen RL. 1999 The electronic states of carotenoids. In *The photochemistry of carotenoids* (eds HA Frank, AJ Young, G Britton, RJ Cogdell), pp. 137–159. Dordrecht, The Netherlands: Springer.
47. Gill D, Kilponen RG, Rimai L. 1970 Resonance Raman scattering of laser radiation by vibrational modes of carotenoid pigment molecules in intact plant tissues. *Nature* **227**, 743–744. (doi:10.1038/227743a0)
48. Saito S, Tasumi M. 1983 Normal-coordinate analysis of retinal isomers and assignments of Raman and infrared bands. *J. Raman Spectrosc.* **14**, 236–245. (doi:10.1002/jrs.1250140405)
49. Koyama Y, Takii T, Saiki K, Tsukida K. 1983 Configuration of the carotenoid in the reaction centers of photosynthetic bacteria. 2. Comparison of the resonance Raman lines of the reaction centers with those of the 14 different cis-trans isomers of β-carotene. *Photobiochem. Photobiophys.* **5**, 139–150.
50. Koyama Y, Fujii R. 1999 Cis-trans carotenoids in photosynthesis: configurations, excited-state properties and physiological functions. In *The photochemistry of carotenoids* (eds HA Frank, AJ Young, G Britton, RJ Cogdell), pp. 161–188. Dordrecht, The Netherlands: Springer.
51. Rimai L, Heyde ME, Gill D. 1973 Vibrational spectra of some carotenoids and related linear polyenes. Raman spectroscopic study. *J. Am. Chem. Soc.* **95**, 4493–4501. (doi:10.1021/ja00795a005)
52. Koyama Y, Kito M, Takii T, Saiki K, Tsukida K, Yamashita J. 1982 Configuration of the carotenoid in the reaction centers of photosynthetic bacteria. Comparison of the resonance Raman spectrum of the reaction center of *Rhodopseudomonas sphaeroides* G1C with those of *cis-trans* isomers of β-carotene. *Biochim. Biophys. Acta* **680**, 109–118. (doi:10.1016/0005-2728(82)90001-9)
53. Koyama Y, Takatsuka I, Nakata M, Tasumi M. 1988 Raman and infrared spectra of the all-*trans*, 7-*cis*, 9-*cis*, 13-*cis* and 15-*cis* isomers of β-carotene: key bands distinguishing stretched or terminal-bent configurations form central-bent configurations. *J. Raman Spectrosc.* **19**, 37–49. (doi:10.1002/jrs.1250190107)
54. Andreeva A, Apostolova I, Velitchkova M. 2011 Temperature dependence of resonance Raman spectra of carotenoids. *Spectrochim. Acta A Mol. Biomol. Spectrosc.* **78**, 1261–1265. (doi:10.1016/j.saa.2010.12.071)
55. Mendes-Pinto MM, Galzerano D, Telfer A, Pascal AA, Robert B, Ilioaia C. 2013 Mechanisms underlying carotenoid absorption in oxygenic photosynthetic proteins. *J. Biol. Chem.* **288**, 18 758–18 765. (doi:10.1074/jbc.M112.423681)
56. Salares VR, Young NM, Carey PR, Bernstein HJ. 1977 Excited state (excitation) interactions in polyene aggregates. Resonance Raman and absorption spectroscopic evidence. *J. Raman Spectrosc.* **6**, 282–288. (doi:10.1002/jrs.1250060605)
57. Lutz M, Szponarski W, Berger G, Robert B, Neumann J-M. 1987 The stereoisomerization of bacterial, reaction-center-bound carotenoids revisited: an electronic absorption, resonance Raman and NMR study. *Biochem. Biophys. Acta* **894**, 423–433. (doi:10.1016/0005-2728(87)90121-6)

58. Wirtz AC, van Hemert MC, Lugtenburg J, Frank HA, Groenen EJJ. 2007 Two stereoisomers of spheroidene in the *Rhodobacter sphaeroides* R26 reaction center: a DFT analysis of resonance Raman spectra. *Biophys. J.* **93**, 981–991. (doi:10.1529/biophysj.106.103473)
59. Dokter AM, van Hemert MC, In't Velt CM, van der Hoef K, Lugtenburg J, Frank HA, Groenen EJJ. 2002 Resonance Raman spectrum of all-trans-spheroidene. DFT analysis and isotope labeling. *J. Phys. Chem. A* **106**, 9463–9469. (doi:10.1021/jp026164e)
60. Kish E, Mendes Pinto MM, Bovi D, Basire M, Guidoni L, Vuilleumier R, Robert B, Spezia R, Mezzetti A. 2014 Fermi resonance as a tool for probing peridinin environment. *J. Phys. Chem. B* **118**, 5873–5881. (doi:10.1021/jp501667t)
61. Macernis M, Galzerano D, Sulskus J, Kish E, Kim Y-H, Koo S, Valkunas L, Robert B. 2015 Resonance Raman spectra of carotenoid molecules: influence of methyl substitutions. *J. Phys. Chem. A* **119**, 56–66. (doi:10.1021/jp510426m)
62. Macernis M, Sulskus J, Malickaja S, Robert B, Valkunas L. 2014 Resonance Raman spectra and electronic transitions in carotenoids: a density functional theory study. *J. Phys. Chem. A* **118**, 1817–1825. (doi:10.1021/jp406449c)
63. Robert B. 2009 Resonance Raman spectroscopy. *Photosynth. Res.* **101**, 147–155. (doi:10.1007/s11120-009-9440-4)
64. Araki G, Murai T. 1952 Molecular structure and absorption spectra of carotenoids. *Prog. Theor. Phys.* **8**, 639–654. (doi:10.1143/PTP.8.639)
65. Dale J. 1954 Empirical relationships of the minor bands in the absorption spectra of polyenes. *Acta Chem. Scand.* **8**, 1235–1256. (doi:10.3891/acta.chem.scand.08-1235)
66. Hemley R, Kohler BE. 1977 Electronic structure of polyenes related to the visual chromophore. A simple model for the observed band shapes. *Biophys. J.* **20**, 377–382. (doi:10.1016/S0006-3495(77)85556-2)
67. Christensen RL, Barney EA, Broene RD, Galinato MGI, Frank HA. 2004 Linear polyenes: models for the spectroscopy and photophysics of carotenoids. *Arch. Biochem. Biophys.* **430**, 30–36. (doi:10.1016/j.abb.2004.02.026)
68. Polívka T, Sundström V. 2004 Ultrafast dynamics of carotenoid excited states—from solution to natural and artificial systems. *Chem. Rev.* **104**, 2021–2072. (doi:10.1021/cr020674n)
69. Merlin JC. 1985 Resonance Raman spectroscopy of carotenoids and carotenoid-containing systems. *Pure Appl. Chem.* **57**, 785–792. (doi:10.1351/pac198557050785)
70. Knoll K, Schrock RR. 1989 Preparation of tert-butyl-capped polyenes containing up to 15 double bonds. *J. Am. Chem. Soc.* **111**, 7989–8004. (doi:10.1021/ja00202a045)
71. Frank HA, Josue JS, Bautista JA, van der Hoef I, Jansen FJ, Lugtenburg J, Wiederrecht G, Christensen RL. 2002 Spectroscopic and photochemical properties of open-chain carotenoids. *J. Phys. Chem. B* **106**, 2083–2092. (doi:10.1021/jp013321l)
72. Wasielewski MR, Kispert LD. 1986 Direct measurement of the lowest excited singlet state lifetime of all-trans-β-carotene and related carotenoids. *Chem. Phys. Lett.* **128**, 238–243. (doi:10.1016/0009-2614(86)80332-3)
73. Frank HA, Desamero RZB, Chynwat V, Gebhard R, van der Hoef I, Jansen FJ, Lugtenburg J, Gosztola D, Wasielewski MR. 1997 Spectroscopic properties of spheroidene analogs having different extents of Π-electron conjugation. *J. Phys. Chem. A* **101**, 149–157. (doi:10.1021/jp962373l)
74. Withnall R, Chowdhry BZ, Silver J, Edwards HGM, de Oliveira LFC. 2003 Raman spectra of carotenoids in natural products. *Spectrochim. Acta A Mol. Biomol. Spectrosc.* **59**, 2207–2212. (doi:10.1016/S1386-1425(03)00064-7)
75. Mendes-Pinto MM, Sansiaume E, Hashimoto H, Pascal AA, Gall A, Robert B. 2013 Electronic absorption and ground state structure of carotenoid molecules. *J. Phys. Chem. B* **117**, 11 015–11 021. (doi:10.1021/jp309908r)
76. Fuciman M, Keşan G, LaFountain AM, Frank HA, Polívka T. 2015 Tuning the spectroscopic properties of aryl carotenoids by slight changes in structure. *J. Phys. Chem. B* **119**, 1457–1467. (doi:10.1021/jp512354r)
77. Fujii R, Inaba T, Watanabe Y, Koyama Y, Zhang J-P. 2003 Two different pathways of internal conversion in carotenoids depending on the length of the conjugated chain. *Chem. Phys. Lett.* **369**, 165–172. (doi:10.1016/S0009-2614(02)01999-1)
78. Christensen RL, Kohler BE. 1973 Low resolution optical spectroscopy of retinyl polyenes: low lying electronic levels and spectral broadness. *Photochem. Photobiol.* **18**, 293–301. (doi:10.1111/j.1751-1097.1973.tb06424.x)
79. Fuciman M, Chabera P, Zupcanova A, Hribek P, Arellano JB, Vacha F, Psencik J, Polivka T. 2010 Excited state properties of aryl carotenoids. *Phys. Chem. Chem. Phys.* **12**, 3112–3120. (doi:10.1039/B921384H)
80. Suzuki H, Mizuhashi S. 1964 Π-electronic structure and absorption spectra of carotenoids. *J. Phys. Soc. Jpn.* **19**, 724–738. (doi:10.1143/JPSJ.19.724)
81. LeRosen AL, Reid CE. 1952 An investigation of certain solvent effect in absorption spectra. *J. Chem. Phys.* **20**, 233–236. (doi:10.1063/1.1700384)
82. Hirayama K. 1955 Absorption spectra and chemical structure. II. Solvent effect. *J. Am. Chem. Soc.* **77**, 379–381. (doi:10.1021/ja01607a042)
83. Andersson PO, Gillbro T, Ferguson L, Cogdell RJ. 1991 Absorption spectral shifts of carotenoids related to medium polarizability. *Photochem. Photobiol.* **54**, 353–360. (doi:10.1111/j.1751-1097.1991.tb02027.x)
84. Kuici M, Nagae H, Cogdell RJ, Shimada K, Koyama Y. 1994 Solvent effect on spheroidene in nonpolar and polar solutions and the environment of spheroidene in the light-harvesting complexes of *Rhodobacter sphaeroides* 2.4.1 as revealed by the energy of the $^1A_g^- \rightarrow {}^1B_u^+$ absorption and the frequencies of the vibronically coupled C=C stretching Raman lines in the $^1A_g^-$ and $^1B_u^-$ states. *Photochem. Photobiol.* **59**, 116–124. (doi:10.1111/j.1751-1097.1994.tb05009.x)
85. Chen Z, Lee C, Lenzer T, Oum K. 2006 Solvent effects on the $S_0(^1Ag^-) \rightarrow S_2(^1Bu^+)$ transition of β-carotene, echinenone, canthaxanthin, and astaxanthin in supercritical CO_2 and CF_3H. *J. Phys. Chem. A* **110**, 11 291–11 297. (doi:10.1021/jp0643247)
86. Renge I, Sild E. 2011 Absorption shifts in carotenoids—influence of index of refraction and submolecular electric fields. *J. Photochem. Photobiol. A* **218**, 156–161. (doi:10.1016/j.jphotochem.2010.12.015)
87. Frank HA, Bautista JA, Josue J, Pendon Z, Hiller RG, Sharples FP, Gosztola D, Wasielewski MR. 2000 Effect of the solvent environment on the spectroscopic properties and dynamics of the lowest excited states of carotenoids. *J. Phys. Chem. B* **104**, 4569–4577. (doi:10.1021/jp000079u)
88. Llansola-Portoles MJ, Uragami C, Pascal AA, Bina D, Litvin R, Robert B. 2016 Pigment structure in the FCP-like light-harvesting complex from *Chromera velia*. *Biochim. Biophys. Acta* **1857**, 1759–1765. (doi:10.1016/j.bbabio.2016.08.006)
89. Kish E, Pinto MMM, Kirilovsky D, Spezia R, Robert B. 2015 Echinenone vibrational properties: from solvents to the orange carotenoid protein. *Biochim. Biophys. Acta* **1847**, 1044–1054. (doi:10.1016/j.bbabio.2015.05.010)
90. Takaichi S. 1999 Carotenoids and carotenogenesis in anoxygenic photosynthetic bacteria. In *The photochemistry of carotenoids* (eds HA Frank, AJ Young, G Britton, RJ Cogdell), pp. 39–69. Dordrecht, The Netherlands: Springer.
91. Angerhofer A, Bornhäuser F, Gall A, Cogdell RJ. 1995 Optical and optically detected magnetic resonance investigation on purple photosynthetic bacterial antenna complexes. *Chem. Phys.* **194**, 259–274. (doi:10.1016/0301-0104(95)00022-G)
92. Ruban AV, Pascal AA, Robert B. 2000 Xanthophylls of the major photosynthetic lightharvesting complex of plants: identification, conformation and dynamics. *FEBS Lett.* **477**, 181–185. (doi:10.1016/S0014-5793(00)01799-3)
93. Caffarri S, Croce R, Breton J, Bassi R. 2001 The major antenna complex of photosystem II has a xanthophyll binding site not involved in light harvesting. *J. Biol. Chem.* **276**, 35 924–35 933. (doi:10.1074/jbc.M105199200)
94. Llansola-Portoles MJ, Sobotka R, Kish E, Shukla MK, Pascal AA, Polívka T, Robert B. 2017 Twisting a β-carotene, an adaptive trick from nature for dissipating energy during photoprotection. *J. Biol. Chem.* **292**, 1396–1403. (doi:10.1074/jbc.M116.753723)
95. Polívka T, Kerfeld CA, Pascher T, Sundström V. 2005 Spectroscopic properties of the carotenoid 3′-hydroxyechinenone in the orange carotenoid protein from the cyanobacterium *Arthrospira maxima*. *Biochemistry* **44**, 3994–4003. (doi:10.1021/bi047473t)
96. Polívka T, Chábera P, Kerfeld CA. 2013 Carotenoid–protein interaction alters the S_1 energy of

hydroxyechinenone in the orange carotenoid protein. *Biochim. Biophys. Acta* **1827**, 248–254. (doi:10.1016/j.bbabio.2012.10.005)

97. Shima S, Ilagan RP, Gillespie N, Sommer BJ, Hiller RG, Sharples FP, Frank HA, Birge RR. 2003 Two-photon and fluorescence spectroscopy and the effect of environment on the photochemical properties of peridinin in solution and in the peridinin-chlorophyll-protein from *Amphidinium carterae*. *J. Phys. Chem. A* **107**, 8052–8066. (doi:10.1021/jp022648z).
98. Premvardhan L, Bordes L, Beer A, Büchel C, Robert B. 2009 Carotenoid structures and environments in trimeric and oligomeric fucoxanthin chlorophyll a/c2 proteins from resonance Raman spectroscopy. *J. Phys. Chem. B* **113**, 12 565–12 574. (doi:10.1021/jp903029g)
99. Büchel C. 2003 Fucoxanthin-chlorophyll proteins in diatoms: 18 and 19 kDa subunits assemble into different oligomeric states. *Biochemistry* **42**, 13 027–13 034. (doi:10.1021/bi0349468)
100. Feng J, Tseng C-W, Chen T, Leng X, Yin H, Cheng Y-C, Rohlfing M, Ma Y. 2017 A new energy transfer channel from carotenoids to chlorophylls in purple bacteria. *Nat. Commun.* **8**, 71. (doi:10.1038/s41467-017-00120-7)
101. Desamero RZB *et al.* 1998 Mechanism of energy transfer from carotenoids to bacteriochlorophyll: light-harvesting by carotenoids having different extents of Π-electron conjugation incorporated into the B850 antenna complex from the carotenoidless bacterium *Rhodobacter sphaeroides* R-26.1. *J. Phys. Chem. B* **102**, 8151–8162. (doi:10.1021/jp980911j)
102. Mattioli TA, Hoffmann A, Sockalingum DG, Schrader B, Robert B, Lutz M. 1993 Application of near-IR Fourier transform resonance Raman spectroscopy to the study of photosynthetic proteins. *Spectrochim. Acta A Mol. Spectrosc.* **49**, 785–799. (doi:10.1016/0584-8539(93)80103-H)
103. McDermott G, Prince SM, Freer AA, Hawthornthwaite-Lawless AM, Papiz MZ, Cogdell RJ, Isaacs NW. 1995 Crystal structure of an integral membrane light-harvesting complex from photosynthetic bacteria. *Nature* **374**, 517–521. (doi:10.1038/374517a0)
104. van Dorssen RJ, Breton J, Plijter JJ, Satoh K, van Gorkom HJ, Amesz J. 1987 Spectroscopic properties of the reaction center and of the 47 kDa chlorophyll protein of photosystem II. *Biochim. Biophys. Acta* **893**, 267–274. (doi:10.1016/0005-2728(87)90048-X)
105. Kwa SLS, Newell WR, van Grondelle R, Dekker JP. 1992 The reaction center of photosystem II studied with polarized fluorescence spectroscopy. *Biochim. Biophys. Acta* **1099**, 193–202. (doi:10.1016/0005-2728(92)90027-Y)
106. Tomo T, Mimuro M, Iwaki M, Kobayashi M, Itoh S, Satoh K. 1997 Topology of pigments in the isolated photosystem II reaction center studied by selective extraction. *Biochim. Biophys. Acta* **1321**, 21–30. (doi:10.1016/S0005-2728(97)00037-6)
107. Kirilovsky D, Kerfeld CA. 2013 The orange carotenoid protein: a blue-green light photoactive protein. *Photochem. Photobiol. Sci.* **12**, 1135–1143. (doi:10.1039/C3PP25406B)
108. Kirilovsky D, Kerfeld CA. 2016 Cyanobacterial photoprotection by the orange carotenoid protein. *Nat. Plants* **2**, 16180. (doi:10.1038/nplants.2016.180)
109. Wilson A, Kinney JN, Zwart PH, Punginelli C, D'Haene S, Perreau F, Klein MG, Kirilovsky D, Kerfeld CA. 2010 Structural determinants underlying photoprotection in the photoactive orange carotenoid protein of cyanobacteria. *J. Biol. Chem.* **285**, 18 364–18 375. (doi:10.1074/jbc.M110.115709)
110. Wilson A *et al.* 2008 A photoactive carotenoid protein acting as light intensity sensor. *Proc. Natl Acad. Sci. USA* **105**, 12 075–12 080. (doi:10.1073/pnas.0804636105)
111. Durchan M *et al.* 2014 Highly efficient energy transfer from a carbonyl carotenoid to chlorophyll *a* in the main light harvesting complex of *Chromera velia*. *Biochim. Biophys. Acta* **1837**, 1748–1755. (doi:10.1016/j.bbabio.2014.06.001)